

TOP QUARK PROPERTIES

TONY M. LISS

Department of Physics

University of Illinois

Urbana, Illinois 61801

E-mail: tml@illinois.edu

On behalf of the CDF, D0, ATLAS and CMS Collaborations

I review the latest results on properties of the top quark from the Tevatron and the LHC, including results measured in $t\bar{t}$ and single-top events on the mass, width, couplings, and spin correlations.

1 Introduction

With results from almost 9 fb^{-1} of $\bar{p}p$ collisions at $\sqrt{s} = 1.96 \text{ TeV}$ at the Tevatron, and up to 5 fb^{-1} of pp collisions at $\sqrt{s} = 7 \text{ TeV}$ at the LHC, measurements of top-quark properties are becoming quite precise. I will review the latest (as of early September, 2012) results from D0 and CDF at the Tevatron and CMS [1] and ATLAS [2] at the LHC. These results include the top quark mass and width, the t and \bar{t} mass difference, top quark couplings, and $t - \bar{t}$ spin correlations. The top quark charge asymmetry is covered elsewhere [3]. The event selection and background evaluation are also covered elsewhere [4].

2 Top Quark Mass Measurements

The top quark's mass, m_t , is its most fundamental property. It is also the most precisely measured property. Besides being a free parameter in the Standard Model, the importance of the top quark mass measurements stems from its role in electroweak radiative corrections which yield a quadratic dependence of the W boson mass, m_W , on m_t , while m_W only depends logarithmically on m_H , the mass of the Higgs boson. Precision measurements of m_W and m_t therefore probe the Standard Model Higgs boson mass, as shown in Figure 1, and with a precise measurement of the Higgs boson mass probe the consistency of the Standard Model itself.

The measurement of m_t involves a number of challenges. The top quark decays almost 100% of the time to a W boson and a b quark. The $t\bar{t}$ final state, $W^+bW^-\bar{b}$ with each W boson decaying to $\ell\nu$ or qq' , involves six partons, and these must be identified in the selected events and properly assigned to the two W bosons and the b and \bar{b} quarks. In addition to the parton assignment, the best possible energy and momentum resolution must be achieved for each, and here the jet energy scale (JES) is of paramount importance.

A large number of techniques have been used over the years for measuring m_t . Here I will discuss only those used in a few of the most recent results.

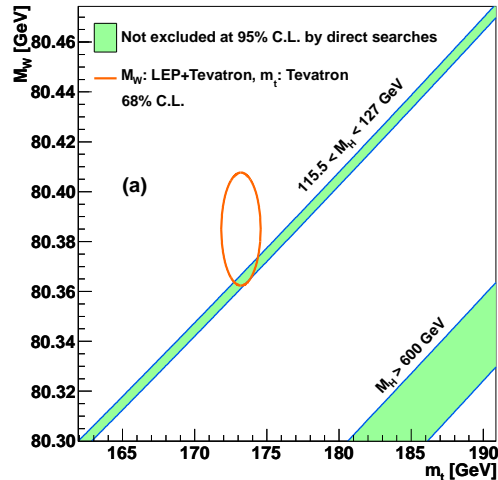


Figure 1. Top mass vs. W boson mass showing bands of Standard Model Higgs boson masses. The ellipse shows the current Tevatron averages. The figure is from Reference [5].

2.1 CDF Measurement in lepton+jets

The CDF collaboration has recently released a measurement in 8.7 fb^{-1} of $p\bar{p}$ collisions at \sqrt{s} in the lepton+jets channel using a template fitting technique [6]. A χ^2 minimization is used to assign measured objects to final-state partons. The reconstructed top mass is a free parameter in the χ^2 , with the constraint that $m_t^{reco} = m_t^{reco}$, and the χ^2 includes resolution terms that allow the measured p_T for each object to vary. The χ^2 is minimized with respect to m_t and the distribution of m_t^{reco} values over the ensemble of events is fit to Monte Carlo templates for the distribution of m_t^{reco} as a function of the true top mass. The JES uncertainty is controlled by a simultaneous fit of m_{jj} from the hadronically decaying W boson to the known W boson mass. The result, shown in Figure 2, is

$$m_t = 172.9 \pm 0.7 \text{ (JES + stat.)} \pm 0.8 \text{ (syst.) GeV}$$

The uncertainty due to JES is included as a statistical uncertainty here due to the m_{jj} fit. This is the most precise single measurement of the top-quark mass to date.

2.2 D0 Measurement in Dileptons

The D0 collaboration has recently measured the top mass in 5.3 fb^{-1} in the dilepton channel ($ee, \mu\mu, e\mu$) [7]. In this channel there are two unobserved neutrinos, resulting in a kinematically under-constrained system. To address this problem

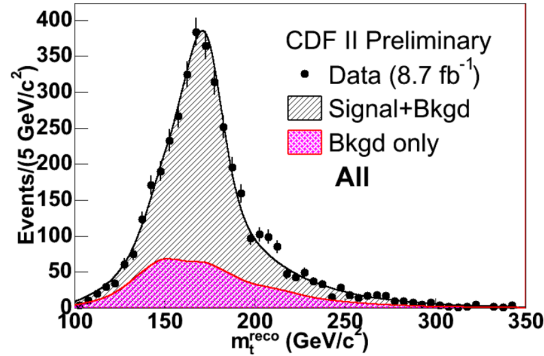


Figure 2. CDF top mass fit in the lepton+jets channel using the template method. The figure is from Reference [6].

three additional constraints are needed. Two are given as follows:

$$\begin{aligned} m(\ell_1\nu_1) &= m(\ell_2\nu_2) = m_W \\ m(\ell_1\nu_1b_1) &= m(\ell_2\nu_2b_2) \end{aligned}$$

There are a number of different choices for imposing the third constraint. In this measurement an integration is performed over the pseudorapidity of both neutrinos, η_1 and η_2 . At each (η_1, η_2) the neutrino momenta are calculated and from them the missing E_T . A weight is assigned based on the agreement between the calculated and measured missing E_T , and the missing E_T resolution. Figure 3 shows the maximum likelihood fit to the weight distribution from which the top mass is extracted. The result is

$$m_t = 174.0 \pm 2.4 \text{ (JES + stat.)} \pm 1.4 \text{ (syst.) GeV}$$

2.3 Tevatron Top Mass Combination

The CDF and D0 collaborations have combined a variety of different measurements of the top quark mass using integrated luminosities up to 5.8 fb^{-1} [5]. The combination does not yet include the latest results, such as those described in Sections 2.1. Figure 4 shows the measurements used in the combination. Taking into account correlations in the systematic uncertainties between the different measurements, the combined top mass value is found to be

$$m_t = 173.18 \pm 0.56 \text{ (stat.)} \pm 0.75 \text{ (syst.) GeV.}$$

The top mass measured from Tevatron data has a precision of 0.54%. A remarkable achievement.

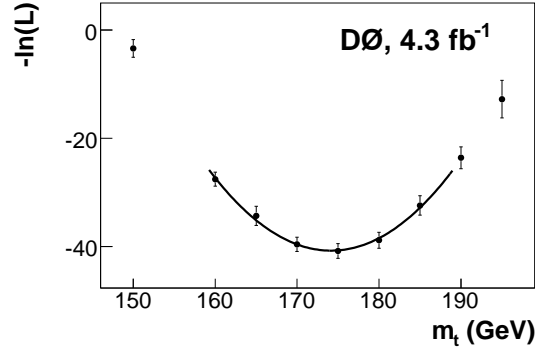


Figure 3. D0 top mass fit in the dilepton channel using the neutrino weighting method. The figure is from Reference [7]. The result quoted in the text is a combination with an earlier 1 fb^{-1} analysis.

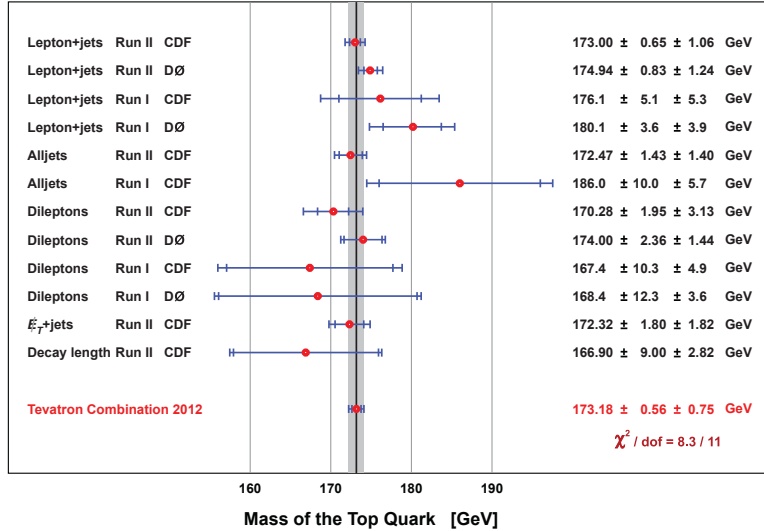


Figure 4. The twelve input measurements of m_t and the combined value from the Tevatron experiments. The figure is from Reference [5].

2.4 ATLAS & CMS Top Mass Measurements

At the LHC at $\sqrt{s} = 7 \text{ TeV}$ the $t\bar{t}$ production cross section is roughly 20 times what it is at the Tevatron. Both ATLAS and CMS have taken advantage of the large number of top quarks to employ new techniques for measuring m_t . Using lepton+jets events, the ATLAS collaboration uses the three jets from hadronic-side top decay to form the per-event ratio R_{32} [8], defined as

$$R_{32} = \frac{m(qqb)}{m(qq)}$$

The jet triplet (qqb) assigned to the hadronic top decay is selected by maximizing a kinematic likelihood. The two jets assigned to the W decay (qq) are constrained to m_W in the likelihood and the JES uncertainty is controlled through the ratio. The top mass is extracted through a maximum likelihood fit of R_{32} templates determined from Monte Carlo simulation for a range of m_t values. Figure 5 shows the template fit result in the μ +jets channel in 1.04 fb^{-1} of data at $\sqrt{s}=7 \text{ TeV}$.

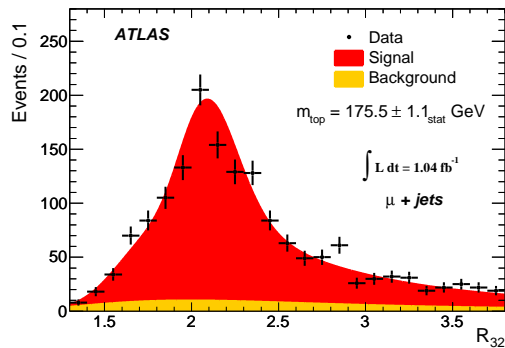


Figure 5. The R_{32} distribution from ATLAS in the μ +jets channel. The crosses show the data with its statistical uncertainty, and the underlying distribution shows the signal and background contributions determined by the fit. The figure is from Reference [8].

An alternate “2-D” method is used by both ATLAS [8] and CMS [9]. In the 2-D method $m(qqb)$ and $m(qq)$ are measured simultaneously (instead of only in ratio). ATLAS does a simultaneous template fit to the *best* assignment, defined as the highest p_T triplet made from a b -tagged jet and light-jet pair with invariant mass between 50 GeV and 100 GeV. In contrast, CMS uses an ideogram method in which *all* jet-parton pairings are used with a weight given by the probability, from Monte Carlo simulation, of the pairing being correct. In both cases the JES is determined by fitting $m(qq)$ to m_W . The distributions of reconstructed m_t are fit to templates. The results are shown in Figure 6.

ATLAS, in 1.04 fb^{-1} of data at $\sqrt{s} = 7 \text{ TeV}$ measures

$$m_t = 174.5 \pm 0.6 \text{ (stat.)} \pm 2.3 \text{ (syst.) GeV,}$$

and CMS in 4.7 fb^{-1} of data at $\sqrt{s} = 7 \text{ TeV}$ measures

$$m_t = 172.6 \pm 0.6 \text{ (stat.)} \pm 1.2 \text{ (syst.) GeV.}$$

There are additional measurements from ATLAS and CMS, including a measurement in the all-jets channel from ATLAS [10], and one in the dilepton channel

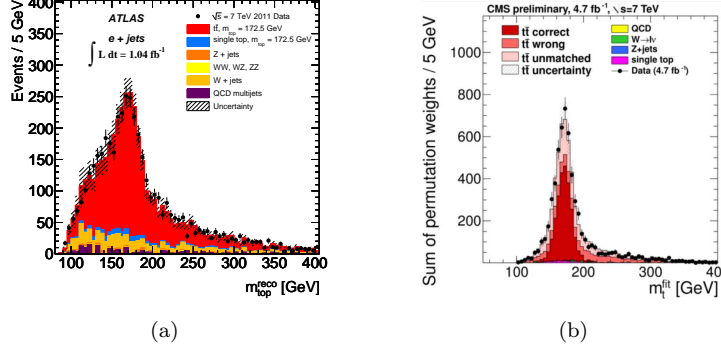


Figure 6. Reconstructed m_t distribution for the *best qqb* assignment from ATLAS (L), and for *all qqb* assignments from CMS (R). The figures are from References [8] and [9].

from CMS [11]. A compilation of the LHC measurements of m_t is shown in Figure 7. The combined m_t value from the LHC is

$$m_t = 173.2 \pm 0.5 \text{ (stat.)} \pm 1.3 \text{ (syst.) GeV.}$$

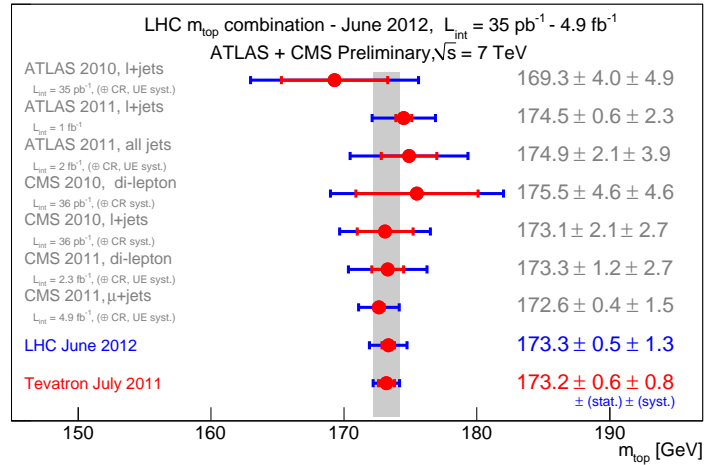


Figure 7. Top mass measurements from the LHC. These results use up to 4.9 fb^{-1} of data taken at $\sqrt{s} = 7 \text{ TeV}$. The figure is from Reference [12], which does not contain the latest results from References [10] and [11].

Separating the lepton+jets data into μ^+ and μ^- events, CMS has measured the top-antitop mass difference [13], which should be zero if CPT is a good symmetry.

The result is

$$\Delta m_t = -0.44 \pm 0.46 \text{ (stat.)} \pm 0.27 \text{ (syst.) GeV}$$

This is the most precise measurement of the mass difference to date. It was first measured by D0 [14] and CDF [15].

3 Top Quark Width and V_{tb}

The production cross section for single-top events is sensitive to the partial width of the top-quark width, $\Gamma(t \rightarrow Wb)$. The D0 collaboration [16] has combined the measured t -channel single-top production cross section and the ratio of top-quark branching fraction, $R = B(t \rightarrow Wb)/B(t \rightarrow Wq)$ to extract the total width of the top quark. The result

$$\Gamma_t = 2.00^{+0.47}_{-0.43} \text{ GeV},$$

for a top mass of 172.5 GeV, is in good agreement with the Standard Model value of 1.3 GeV. The measured result is translated into a top-quark lifetime of $\tau_t = (3.29^{+0.90}_{-0.63}) \times 10^{-25} \text{ s}$.

Since the CKM element V_{tb} and the partial width are proportional to one another, V_{tb} can be extracted by comparison of the measured and predicted (using $V_{tb} \simeq 1.0$) single-top production cross sections. This has been done by all four experiments [17] with results consistent with 1.0 and precision of order 10%.

4 Top-Quark Couplings

In this section I discuss recent results on the top quark electric charge, couplings to W and Z bosons, the W helicity in top-quark decays and searches for flavor-changing-neutral-currents.

4.1 Top-Quark Electroweak Couplings

The top-quark electroweak couplings include those to photons and W and Z bosons. The coupling to photons is sensitive to the electric charge of the top-quark (which is also measured directly at both the Tevatron and LHC using jet-charge techniques). In 1.04 fb^{-1} of data at $\sqrt{s} = 7 \text{ TeV}$, ATLAS has measured the cross section for $t\bar{t}\gamma$ production [18] with a photon p_T threshold of 8 GeV. The result is $\sigma_{t\bar{t}\gamma} = 2.0 \pm 0.5 \text{ stat.} \pm 0.7 \text{ syst.} \pm 0.8 \text{ lumi. pb}$. This compares well with the Standard Model expectation of $2.1 \pm 0.4 \text{ pb}$ for a charge $2/3$ top-quark. There are also direct measurements of the top-quark charge using jet-charge techniques. These are discussed elsewhere in these proceedings [19].

The associated production of $t\bar{t}$ and W or Z bosons has been measured by CMS using trilepton events ($t\bar{t}Z$) and same-sign dilepton events ($t\bar{t}Z$, $t\bar{t}W$) in 4.98 fb^{-1} of pp collisions at $\sqrt{s} = 7 \text{ TeV}$ [20]. The results, compared with the Standard Model predictions, are shown in Figure 8.

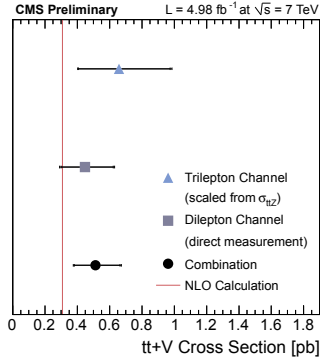


Figure 8. Measurement of the $t\bar{t}V$ production cross section: the cross section from the tripleton channel (blue triangle), from the same sign dilepton channel (grey square) and the combination of the two measurements (black circle) are compared to the NLO calculation (red line). Internal error bars for the measurements represent the statistical component of the uncertainty. The figure is from Reference [20].

4.2 W -boson Helicity

Measurements of the W -boson helicity in top quark decays probe the structure of the Wtb vertex which, in the Standard Model, is $V - A$. For the Standard Model coupling, the fraction of longitudinally polarized W bosons is a function of the top quark and W boson masses, given in the limit of $m_b = 0$ by

$$F_0 = \frac{m_t^2/2m_W^2}{1 + m_t^2/2m_W^2}$$

which gives 69.9% for $m_t = 173.3$ and $m_W = 80.399$. The remainder is almost entirely left-handed. Even with a non-zero m_b the right-handed fraction is tiny.

The measurement of the helicity fractions is based on the angular distribution of the W boson decay products. Figure 9 shows the ideal angular distributions for the three helicity states and their expected Standard Model sum. The angle $\cos\theta^*$ is the charged lepton angle with respect to the top-quark direction in the W rest frame.

The measurement can be made in all top-quark decay channels and is done using a variety of techniques. D0 uses a template fit to the reconstructed angular distributions in a combination of lepton+jets and dileptons $t\bar{t}$ decays in 5.4 fb^{-1} [21]. CDF has used a matrix element technique in 8.7 fb^{-1} [22] of lepton+jets events, that uses the full event kinematics to calculate an event probability as a function of the longitudinal and right-handed helicity fractions. At the LHC, both CMS and ATLAS have made measurements using template fits to the $\cos\theta^*$ distributions in 2.2 fb^{-1} [23] of lepton+jets events and 1.04 fb^{-1} [24] of lepton+jets and dilepton events, respectively. W helicity measurements are made either as two-parameter fits, or one-parameter fits with one helicity fraction fixed to its Standard Model value and $F_0 + F_R + F_L = 1.0$ assumed. A selection of recent results are summarized in Table 1.

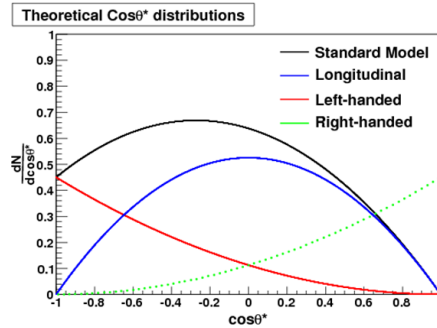


Figure 9. Angular distributions from longitudinal, right-handed and left-handed W bosons. The figure is courtesy of CDF.

Experiment	Helicity	Result	Channel	Reference
D0	F_0	$0.669 \pm 0.078 \pm 0.065$	Dil & LJ	[21]
	F_R	$0.023 \pm 0.041 \pm 0.034$		
CDF	F_0	$0.726 \pm 0.066 \pm 0.067$	LJ	[22]
	F_R	$0.045 \pm 0.043 \pm 0.058$		
CMS	F_0	$0.567 \pm 0.074 \pm 0.047$	LJ	[23]
	F_L	$0.393 \pm 0.045 \pm 0.029$		
ATLAS	F_0	$0.67 \pm 0.03 \pm 0.06$	Dil & LJ	[24]
	F_L	$0.32 \pm 0.02 \pm 0.03$		
	F_R	$0.01 \pm 0.01 \pm 0.04$		

Table 1. Recent measurements of the W boson helicity fractions in top-quark decays. The notation for the $t\bar{t}$ decay channels is ‘Dil’ for the dilepton channel and ‘LJ’ for the lepton+jets channel. The uncertainties listed are statistical and systematic, respectively.

4.3 Searches For Flavor-Changing Neutral Currents

In the Standard Model Flavor-changing neutral current (FCNC) interactions are forbidden at tree level and highly suppressed at higher order by the GIM mechanism. Any observation, therefore, would be a sure sign of physics beyond the Standard Model. Several models of physics beyond the Standard Model predict FCNC effects in top-quark interactions at the 10^{-4} level. The most sensitive tests in the top-quark sector come from single top-quark production in which FCNC production diagrams, such as those shown in Figure 10, modify the production kinematics. Searches in single top-quark production are only sensitive to a tqg coupling.

The first branching fraction limits from single top-quark production came from CDF [25] and D0 [26]. The most precise limits which, taking advantage of the

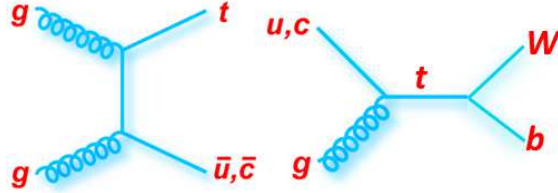


Figure 10. Feynman diagrams for single-top quark production via flavor-changing neutral currents.

relatively large production cross section at the LHC, come from ATLAS [27], are

$$B(t \rightarrow ug) < 5.7 \times 10^{-5}$$

$$B(t \rightarrow cg) < 2.7 \times 10^{-4}$$

Direct searches for $t \rightarrow Zq$ FCNC top-quark decays have been mounted by all four experiments, using final-state kinematics to search for a signal. The most precise limits again come from the LHC, due to the large $t\bar{t}$ production cross section. Both CMS [28] and ATLAS [29] have searched for trileptons in $t\bar{t}$ lepton+jets candidate events, with a same-flavor, opposite-sign pair consistent with a $Z \rightarrow \ell^+\ell^-$ decay. In 2.1 fb^{-1} ATLAS sets a limit of $B(t \rightarrow Zq) < 0.73\%$. In 4.6 fb^{-1} , the CMS limit is $B(t \rightarrow Zq) < 0.34\%$.

5 Top Quark Production Properties

The production cross section for $t\bar{t}$ pairs and for single top-quark production are covered elsewhere in these proceedings [4], as is the $t\bar{t}$ charge asymmetry [3]. Here I concentrate on the top quark spin direction at production.

The top-quark lifetime is so short that, unlike other quarks, it decays before hadronization. As a result, its spin direction at production is preserved through its decay and measurable through the angular distributions of its decay products.

5.1 Top Quark Polarization

The production of $t\bar{t}$ pairs occurs through the strong interaction and therefore, apart from small electroweak corrections, the top-quark spin is expected to be unpolarized. The first study of top-quark polarization was made by D0 at the Tevatron [31]. The CMS experiment has recently measured the polarization of top-quark pairs produced at the LHC [30] using 5.0 fb^{-1} of dilepton events. The polarization angle, θ_ℓ^+ , is defined as the angle between the direction of the positively-charged lepton, in the rest frame of its parent top quark, and the parent top-quark direction in the $t\bar{t}$ rest frame. The measurement of the polarization angle requires a reconstruction of the $t\bar{t}$ system, which is done using an analytic technique. The background subtracted, unfolded distribution is shown in Figure 11.

The polarization, P_n is calculated from the asymmetry of the number of events with positive vs. negative values of $\cos \theta_\ell^+$ and found to be

$$P_n = -0.009 \pm 0.029 \pm 0.041.$$

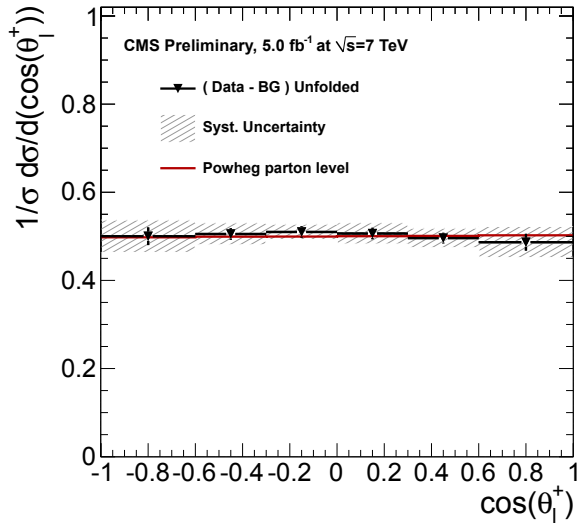


Figure 11. Background-subtracted and unfolded $\cos(\theta_1^+)$ distribution with statistical error bars only. The systematic uncertainty is given by the hatched area. The bin values are correlated due to the unfolding. The figure is from Reference [30].

5.2 $t\bar{t}$ Spin Correlations

While the top-quark spins are unpolarized, they are expected to be correlated. At the Tevatron, where the dominant production mode for $t\bar{t}$ pairs is $q\bar{q}$ annihilation, t and \bar{t} are expected to be produced mostly with opposite helicities. At the LHC, where the production mode is dominantly gluon-gluon annihilation, the $t\bar{t}$ pairs are expected to be like-helicity at low $m_{t\bar{t}}$ and opposite-helicity at high $m_{t\bar{t}}$.

The first results have come from the Tevatron. CDF measures the correlation in the beam basis, where the angles θ^+ and θ^- are defined as the positive and negative lepton directions with respect to the beam direction in the parent top rest frame. Here the double-differential angular distribution is given by

$$\frac{1}{\sigma} \frac{d^2\sigma}{d\cos\theta^+ d\cos\theta^-} = \frac{1 + \kappa \cos\theta^+ \cos\theta^-}{4}$$

CDF uses 5.1 fb^{-1} of dilepton events [32] and a maximum likelihood technique to reconstruct the events, to measure $\kappa = 0.043_{-0.562}^{+0.563}$.

D0 uses a matrix element technique in 5.3 fb^{-1} [33] in which a discriminant R is calculated for each event, where $R = \varphi(\text{corr})/[\varphi(\text{corr}) + \varphi(\text{uncorr})]$ and $\varphi(\text{corr}, \text{uncorr})$ are the matrix-element probabilities for correlated and uncorrelated spins. The distribution of R is fit with templates for correlated and uncorrelated spins to find a fraction of correlated spins of $f = 0.85 \pm 0.29$, yielding the first 3.1σ evidence for spin correlations. Earlier studies from D0 can be found in Ref. [34].

At the LHC, the dominance of the gluon-gluon fusion production of $t\bar{t}$ pairs provides a straightforward technique for measuring the spin correlation. In production

via gluon-gluon fusion, the spin correlation is encoded in the angular separation of the two leptons, $\Delta\phi_{\ell^+\ell^-}$, in dilepton decays of the $t\bar{t}$ pair [35]. Figure 12 shows the data and fits from both ATLAS and CMS.

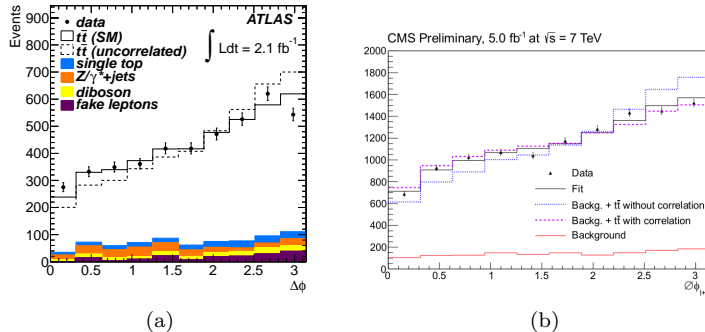


Figure 12. Azimuthal separation between the two leptons in $t\bar{t}$ dilepton decays from ATLAS (a) and CMS (b). The figures are from References [36] and [37].

The data are fit to a sum of the expected distribution for correlated spins and the expected distribution for uncorrelated spins. The ATLAS result is $f = 1.30 \pm 0.14^{+0.27}_{-0.22}$, where the first uncertainty is statistical and the second systematic, and f is the fraction of events with a Standard Model spin correlation. The result excludes $f = 0$ at the 5.1σ level. CMS measures $f = 0.74 \pm 0.08 \pm 0.24$. CMS has also searched for signs of new physics in the dependence of $\Delta\phi_{\ell^+\ell^-}$ on $m_{t\bar{t}}$. Data at both low and high ($> 450 \text{ GeV}$) $m_{t\bar{t}}$ are consistent with Standard Model expectations. CMS also presents results on the asymmetry A_{c1c2} defined as the fraction of events with the product $\cos\theta^+ \times \cos\theta^-$ positive minus the fraction with that product negative. This result requires reconstruction of the $t\bar{t}$ frame in dilepton events and unfolding to correct for detector effects. It is, however, also sensitive to spin correlation in $q\bar{q}$ production of $t\bar{t}$ pairs. While less precise than the measurement of f , the measured value is also consistent with Standard Model expectations.

6 Conclusions

With as much as 9 fb^{-1} of data from the Tevatron, and as much as 5 fb^{-1} analyzed and at least three times that much still to come from the LHC, the era of precision top physics is upon us. I have reviewed the latest results from the four experiments on the top-quark mass, couplings, and searches for rare decay modes. All results are, so far, consistent with Standard Model predictions. As more data are analyzed, and new techniques employed, the precision of these measurements, and sensitivity to beyond-the-Standard-Model effects, will continue to increase.

Acknowledgements

I thank the members of the CDF, D0, ATLAS, and CMS collaborations for the hard work in producing these results and the Fermilab and CERN staff whose outstanding work on the Tevatron and the LHC have produced such rich datasets. This work was supported in part by the U.S. Department of Energy.

References

1. CMS Collaboration, JINST **3** S08004 (2008).
2. ATLAS Collaboration, JINST **3** S08003 (2008).
3. Yvonne Peters, these proceedings.
4. Andreas Meyer, these proceedings.
5. T. Aaltonen, V.M Abazov, *et al.*, The CDF and D0 collaborations., Phys. Rev. **D86**, 092003 (2012); arXiv:1207.1069 (2012).
6. The CDF collaboration., CDF Note 10761.
7. V.M. Abazov *et al.*, The D0 collaboration, Phys. Rev. D **86**, 051103(R) (2012).
8. ATLAS collaboration, Eur.Phys.J. **C72**, 2046 (2012).
9. CMS collaboration, CMS-PAS-TOP-11-015.
10. ATLAS collaboration, ATLAS-CONF-2012-030.
11. CMS collaboration, arXiv:1209.2393. Submitted to EPJC.
12. CMS collaboration, CMS-PAS-TOP-12-001
ATLAS collaboration, ATLAS-CONF-2012-095.
13. CMS collaboration, arXiv:1204.2807. Submitted to JHEP.
14. V.M. Abazov *et al.*, The D0 collaboration, Phys. Rev. Lett. **103**, 132001 (2009)
V.M. Abazov *et al.*, The D0 collaboration, Phys. Rev. D **84**, 052005 (2011).
15. T. Aaltonen *et al.*, The CDF collaboration, Phys. Rev. Lett. **106**, 152001 (2011).
16. V.M. Abazov *et al.*, The D0 collaboration, Phys. Rev. D **85**, 091104 (2012).
17. ATLAS collaboration, Phys. Lett. **B717**, 330 (2012)
CMS collaboration, CMS-PAS-TOP-11-021
CDF collaboration, CDF 10793
D0 collaboration Phys. Rev. **D84**, 112001 (2011)
CDF and D0 collaborations, Fermilab-TM-2440-E.
18. ATLAS collaboration, ATLAS-CONF-2010-153.
19. Pavol Federic, these proceedings.
20. CMS collaboration, CMS-PAS-TOP-12-014.
21. V.M. Abazov *et al.*, The D0 collaboration, Phys. Rev. D **83**, 032009 (2011).
22. CDF collaboration, CDF 10855.
23. CMS collaboration, CMS-PAS-TOP-11-020.
24. ATLAS collaboration, JHEP **1206**, 088 (2012).
25. T. Aaltonen *et al.*, The CDF collaboration, Phys. Rev. Lett. **102**, 151801 (2009).
26. V.M. Abazov *et al.*, The D0 collaboration, Phys.Lett. **B693**, 81 (2010).
27. ATLAS collaboration, Phys. Lett. **B712**, 351 (2012).

28. CMS collaboration, CMS-PAS-TOP-11-028, arXiv:1208.0957.
29. ATLAS collaboration, JHEP **1209**, 139 (2012).
30. CMS collaboration, CMS-PAS-TOP-12-016.
31. V. M. Abazov *et al.* The D0 Collaboration, arXiv:1207.0364.
32. CDF collaboration, CDF 10719.
33. V.M. Abazov, *et al.*, Phys. Rev. Lett. **108**, 032004 (2012).
34. V.M. Abazov, *et al.*, Phys. Rev. Lett. **107**, 032001 (2011)
V.M. Abazov, *et al.*, Phys. Lett. **B702**, 16 (2011).
35. G. Mahlon & S. Parke, Phys. Rev. **D81**, 074024 (2010).
36. ATLAS collaboration, Phys. Rev. Lett. **108**, 212001 (2012).
37. CMS collaboration, CMS-PAS-TOP-12-004.